

## **Synergistic Engineering of Buried Interfaces for High-Efficiency and Stable Perovskite Solar Cells**

Yikun Hua,<sup>‡a</sup> Xinyue Song,<sup>‡a</sup> Lei Zhao,<sup>a</sup> Chao Wu,<sup>a</sup> Jie Zhang,<sup>a</sup> Weiyuan Chen,<sup>a</sup> and Lin Song<sup>\*a</sup>

<sup>a</sup>Frontiers Science Center for Flexible Electronics (FSCFE), Institute of Flexible Electronics (IFE), Northwestern Polytechnical University, 127 West Youyi Road, Xi'an 710072, PR China

<sup>b</sup>Shanghai Synchrotron Radiation Facility (SSRF), Shanghai Advanced Research Institute, Chinese Academy of Sciences, 239 Zhangheng Road, Shanghai 201204, PR China

<sup>‡</sup> These authors contributed equally.

## Experimental detail

### 1. Materials

All materials were used as received without further purified. Fluorine-doped tin oxide (ITO) substrates were purchased from Advanced Election Technology CO., Ltd. Polyethylene naphthalate two formic acid glycol ester (PEN) substrates were purchased from Sunyo Solar Energy Technology Co., Ltd. P-toluenethiol, lead iodide, cesium iodide, molybdenum trioxide ( $\text{MoO}_3$ ), methylammonium chloride (MACl) and methylammonium lead bromide ( $\text{MAPbBr}_3$ ) were purchased from TCI. 2-phenylethylamine hydroiodide (PEAI), formamidinium iodide (FAI) and methylammonium iodide (MAI) were purchased from Great Cell Solar. Chlorobenzene (CB), anisole, anhydrous ethanol, ethyl acetate (EA), N, N-dimethylformamide and dimethyl sulfoxide were purchased from Sigma. 2,2,7,7-Tetrakis [N, N-di (4-methoxyphenyl) amino]-9,9-spirobifluorene (Spiro-OMeTAD) was purchased from Xi'an Yuri Solar Co., Ltd.

### 2. Device fabrication

Glass/ITO and PEN/ITO sheets were cleaned sequentially with ethanol, deionized water and isopropanol for 10 min and then treated with UV-ozone for 20 min.  $\text{SnO}_2$  solution was spin-coated onto ITO or PEN/ITO substrates at 3000 rpm for 30 seconds, followed by annealing at  $150^\circ\text{C}$  for 1 h. Then  $\text{SnO}_2$  substrate were transferred to a glove box for spin-coating p-toluenethiol at 3000 rpm for 30 s after UV-ozone treatment for 20 min.

The annealing process was carried out at  $100^\circ\text{C}$  for 10 min after spin-coating the DMSO solution of p-toluenethiol. Afterward, the perovskite films were deposited by a two-step process using 1.4 M  $(\text{FA}_{0.97}\text{Cs}_{0.03})\text{PbI}_3)_{0.975}(\text{MAPbBr}_3)_{0.025}$  precursor solution, which was spin-coated at 1000 rpm for 10 s, then 4000 rpm for 30 s. Secondly, 150  $\mu\text{L}$  EA was added dropwise at 15 s before the end of the second spin-coating step. After spin coating process, the obtained films were annealed at  $100^\circ\text{C}$  for 40 min, followed by spin-coating PEA solution at 4000 rpm for 30 s. The films were then annealed at  $100^\circ\text{C}$  for 5 min. Subsequently, SpiroO-MeTAD ( $73.2\text{ mg mL}^{-1}$  dissolved in CB) was spin coated on top of the perovskite layer to form a hole transport layer (4000 rpm for 30 s). The oxidation duration of Spiro-OMeTAD was 20 h in a drying cabinet with a relative humidity of 5 %. Finally,  $\text{MoO}_3$  (10 nm) and Ag (100 nm) were thermally evaporated in sequence at a low pressure of  $5.0 \times 10^{-4}$  Pa to complete the perovskite solar cell. The effective area of the device was  $0.05\text{ cm}^2$ . Ten devices were fabricated for each sample group.

### 3. Characterizations

XRD measurements were carried out using a Bruker D8 equipped with a Cu-K $\alpha$  diffractometer. UV/Vis absorption spectra were obtained using U-3900H. High-resolution SEM measured by a field emission GeminiSEM300 model. An optical parametric amplifier (Orpheus, Light Conversion Ltd.) was used to generate a 600 nm pump beam with a standard power density of 50  $\mu\text{J cm}^{-2}$ . A yttrium aluminum garnet crystal was utilized to generate continuous white light pulses (450–950 nm) as probe pulses. TRPL and PL measurements were performed on a FLS100, with an excitation wavelength of 450 nm. Current-voltage characteristic measurements were performed using an AM 1.5G (100  $\text{mW cm}^{-2}$ ) solar simulator (Inergy SS-F5-3A) and a CASE 2400 sourcemeter unit. The J-V scans were carried out by scanning the voltage from 1.4 to  $-0.2$  V (forward scan) and then from  $-0.2$  to 1.4 V (reverse scan) with a step of 0.01 V and a dwell time of 10 ms.

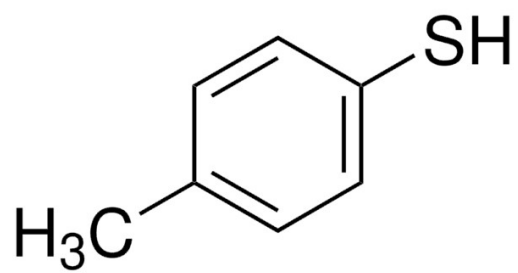


**Figure S1** The chemical structure of p-toluenethiol.

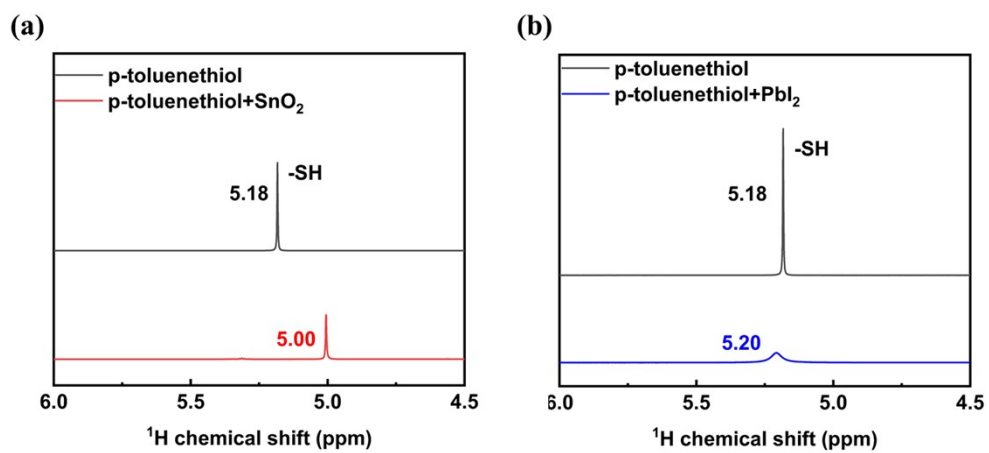


**Figure S2**  $^1\text{H}$  NMR spectra for (a) p-toluenethiol with  $\text{SnO}_2$  and (b) p-toluenethiol with  $\text{PbI}_2$ .

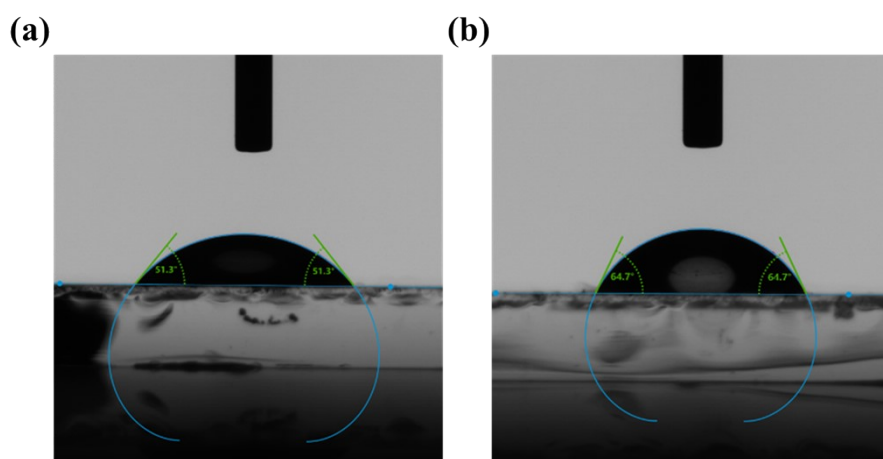
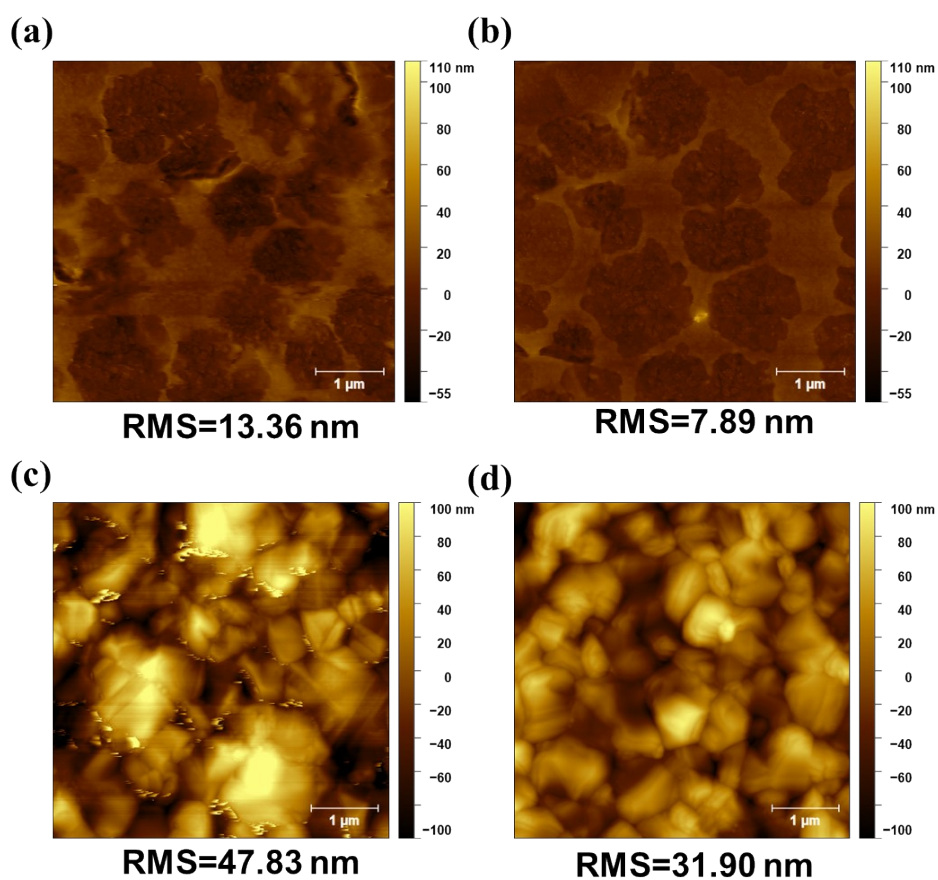


**Figure S3** Water contact angles of (a) ITO/SnO<sub>2</sub> and (b) ITO/SnO<sub>2</sub>/p-toluenethiol.



x

**Figure S4** AFM surface topography images of (a) bare SnO<sub>2</sub> and (b) p-toluenethiol-modified SnO<sub>2</sub> ETLs, and the perovskite films deposited on (c) bare SnO<sub>2</sub> and (d) p-toluenethiol-modified SnO<sub>2</sub> ETLs.

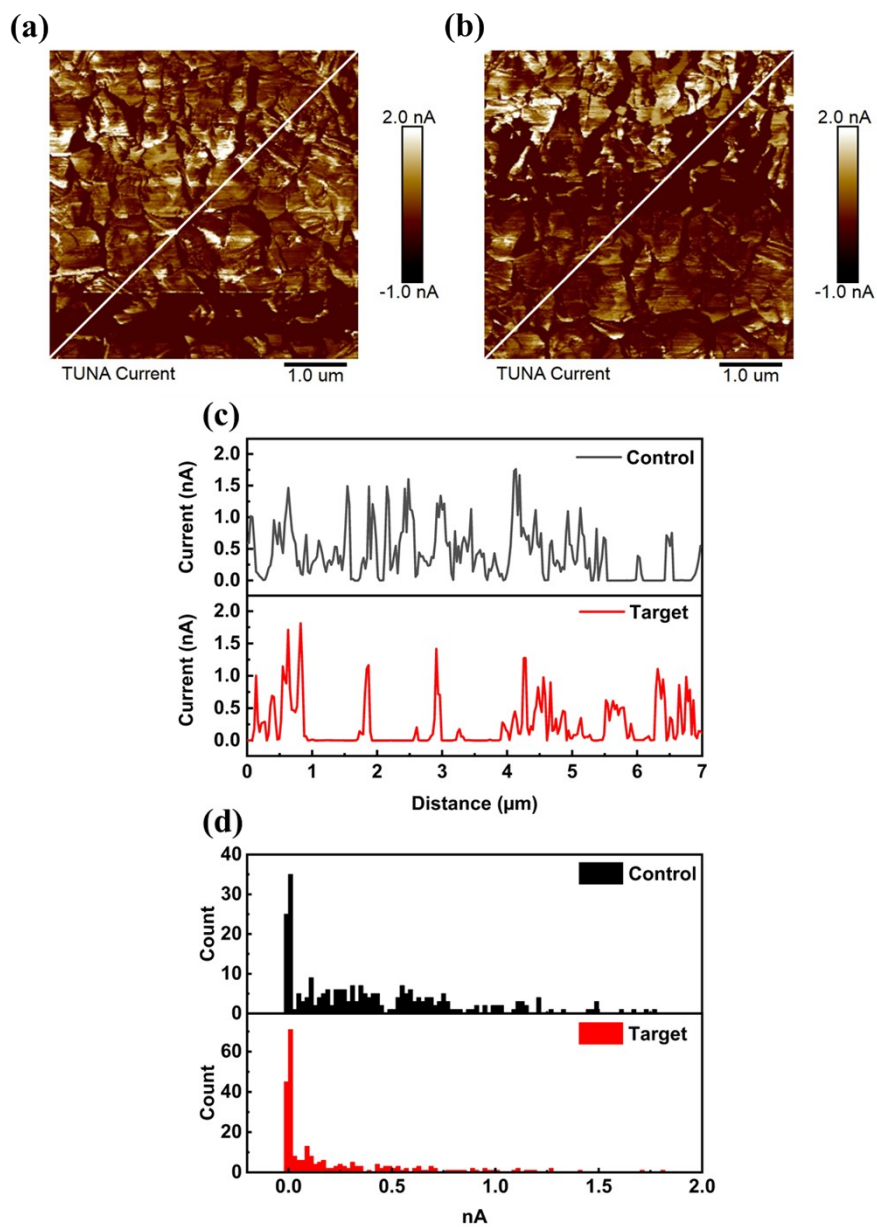


**Figure S5** C-AFM current map of buried interface for (a) the pristine and (b) modified perovskite films. (c) The C-AFM line profiles extracted from Figure S5a and Figure S5b. (d) The statistics of the C-AFM map data extracted from Figure S5c.

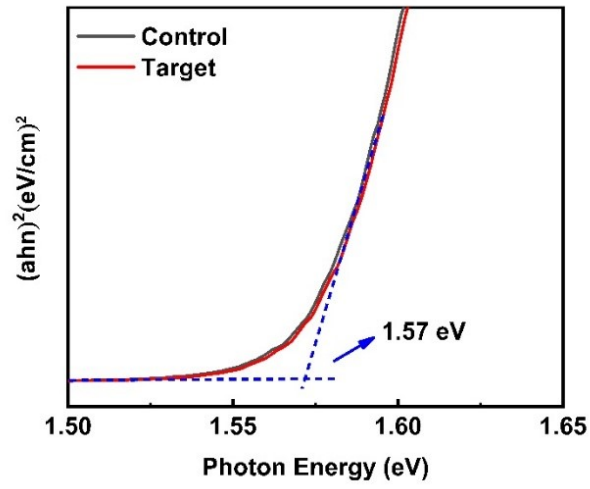


**Figure S6** Tauc plots of perovskite films deposited on the SnO<sub>2</sub> ETLs without and with p-toluenethiol modification.

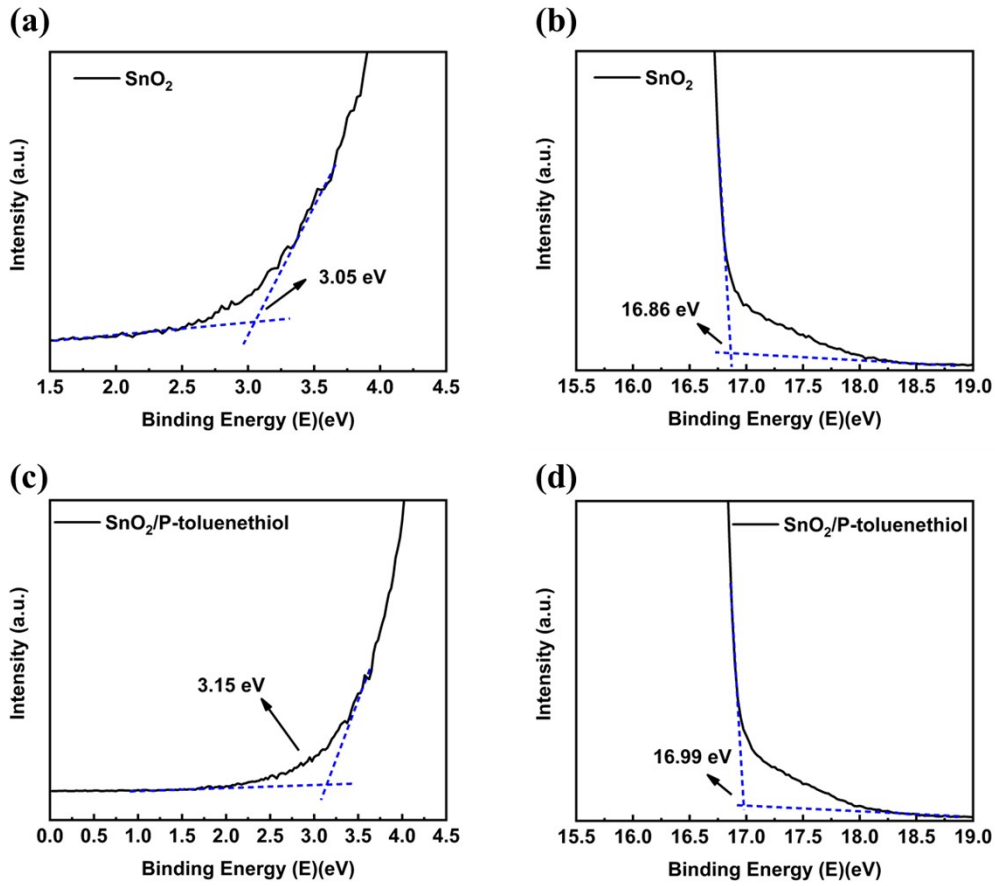


**Figure S7** UPS spectra of (a) valence band and (b) secondary electron cutoff for bare SnO<sub>2</sub>; (c) valence band and (d) secondary electron cutoff for the p-toluenethiol-modified SnO<sub>2</sub>.

Note: To characterize the Fermi level ( $E_F$ ), Valence Band Maximum (VBM) and Conduction Band Minimum (CBM) of the ETLs and perovskite layers, UPS and UV-vis spectra are measured. The  $E_F$  of the samples are derived by subtracting the binding energies of the secondary electron cut-off regions ( $E_{cutoff}$ ) from the excitation photon energy of the He I band (21.22 eV). In the valence band curves, the extracted values ( $E_{gap}$ ) indicate the energy gap between  $E_F$  and VBM. Thus, the  $E_F$ , VBM and CBM can be calculated using the following equations:

$$E_F = -(21.22 - E_{cutoff})$$

$$VBM = E_F - E_{gap}$$

$$CBM = VBM + E_g$$

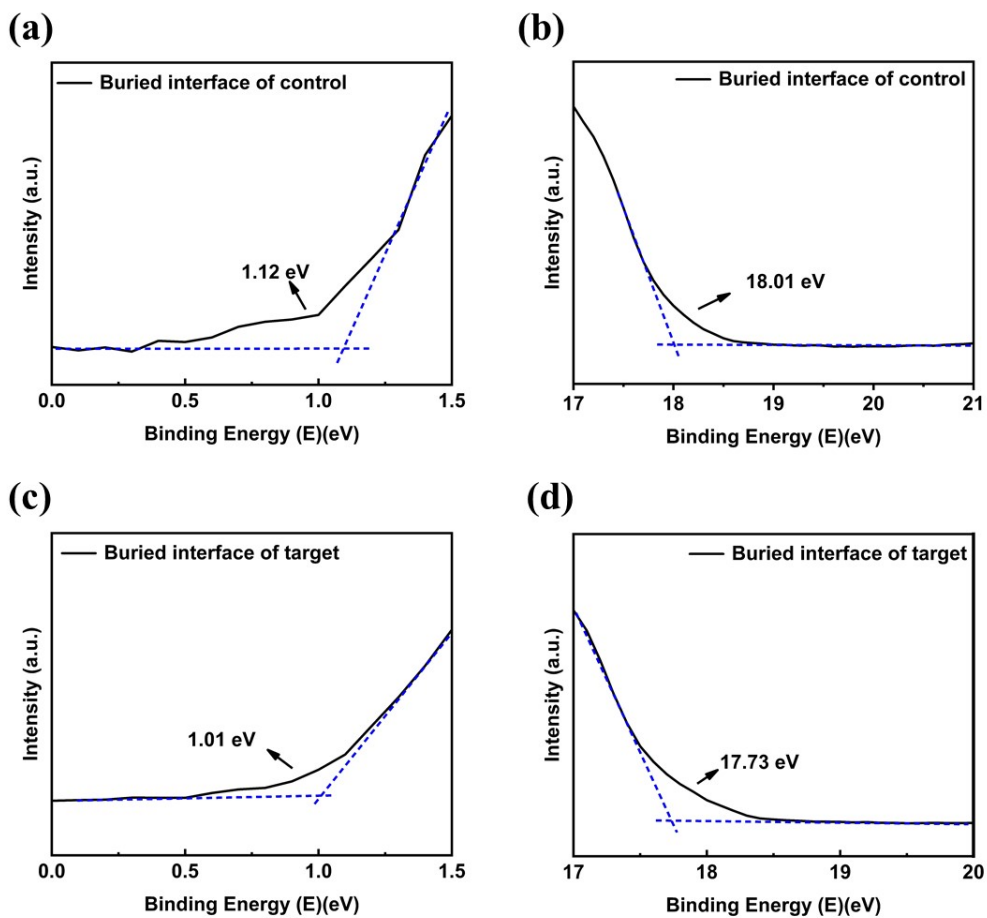


**Figure S8** UPS spectra of (a) valence band and (b) secondary electron cutoff of the buried interface for the control films. (c) valence band and (d) secondary electron cutoff of the buried interface for the p-toluenethiol-modified films.

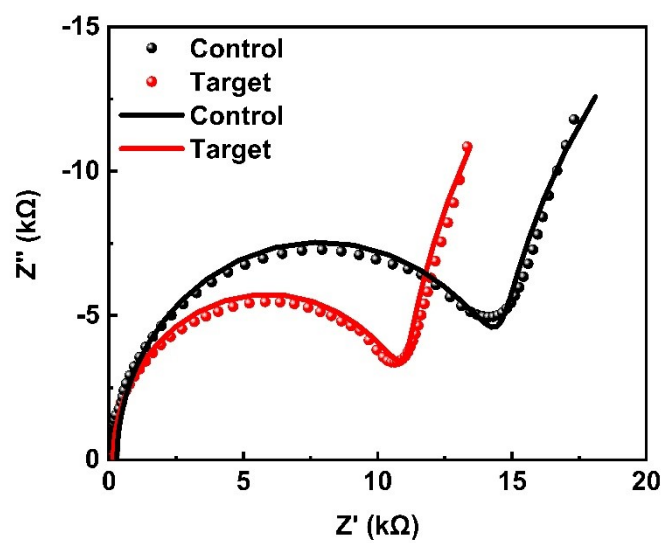


**Figure S9** Nyquist plots of PSCs before and after p-toluenethiol modification. Solid lines represent the fitting.

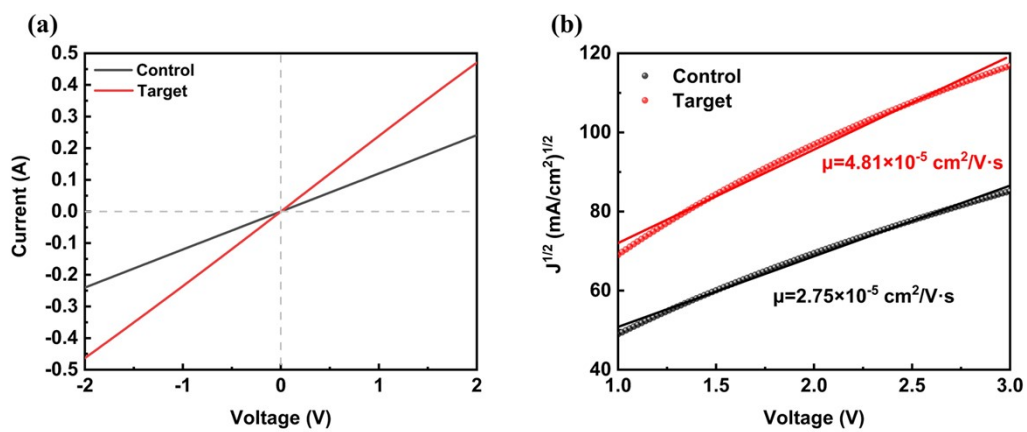


**Figure S10** (a) Current–voltage curves of devices with the structure of ITO/SnO<sub>2</sub>/Ag (Control) or ITO/SnO<sub>2</sub>/ p-toluenethiol/Ag (Target). (b) The related  $J^{1/2}$ –V curves.

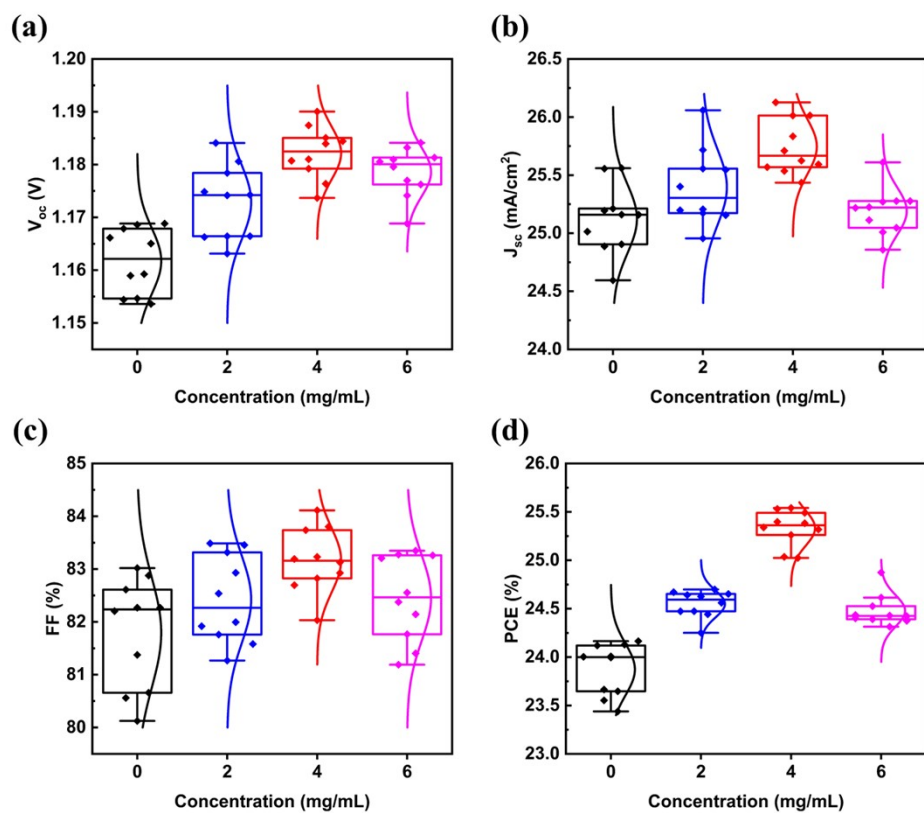


**Figure S11** Statistics of (a)  $V_{OC}$ , (b)  $J_{SC}$ , (c) FF, and (d) PCE based on 10 devices with different concentrations of p-toluenethiol modification.

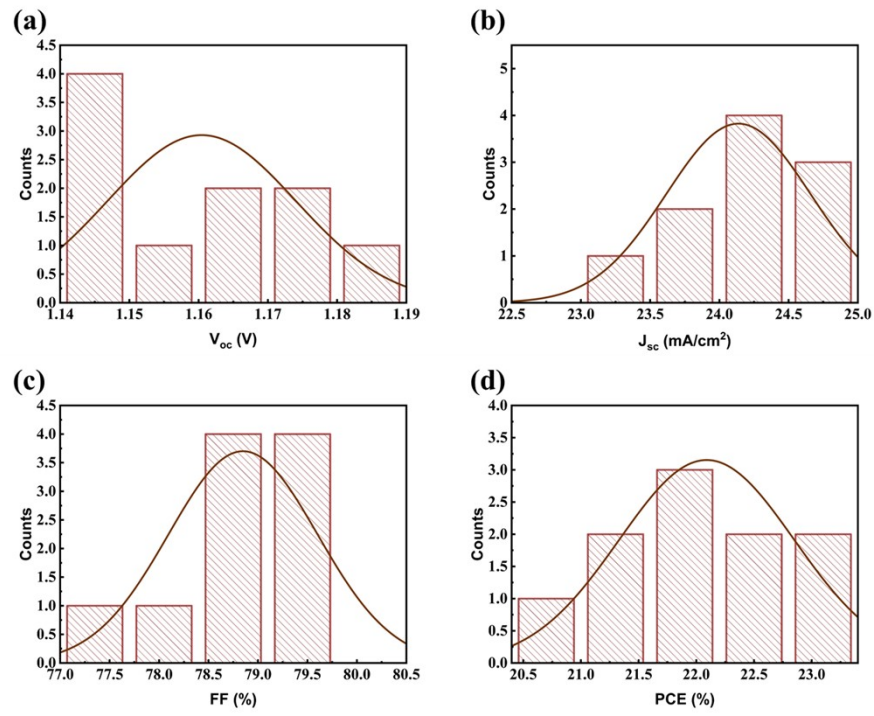


**Figure S12** Statistics of (a)  $V_{OC}$ , (b)  $J_{SC}$ , (c) FF, and (d) PCE based on 10 flexible PSCs.

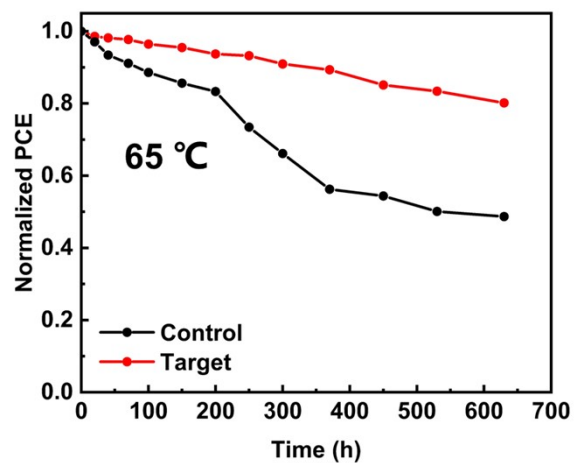


**Figure S13** Thermal stability of PSCs aged in a nitrogen glove box at 65 °C.

**Table S1** Fitting results of the TRPL spectra using bi-exponential equations

Sample	$\tau_1$ (ns)	$A_1$	$\tau_2$ (ns)	$A_2$	$\tau_{ave}$
SnO <sub>2</sub> /Perovskite	275.67	665.33	1396.78	1998.29	1327.65
SnO <sub>2</sub> /P-toluenethiol/Perovskite	53.89	1990.7	612.95	1047.09	532.89

**Table S2** Average photovoltaic parameters and standard deviation of different devices

Sample	$V_{oc}$ (V)	$J_{sc}$ (mA/cm <sup>2</sup> )	FF (%)	PCE (%)
Modified devices	$1.182 \pm 0.005$	$25.74 \pm 0.24$	$83.17 \pm 0.61$	$25.33 \pm 0.18$
Control devices	$1.162 \pm 0.006$	$25.12 \pm 0.30$	$81.80 \pm 1.04$	$23.872 \pm 0.27$
Flexible devices	$1.160 \pm 0.014$	$24.14 \pm 0.52$	$78.85 \pm 0.76$	$22.09 \pm 0.76$